Heat Transfer of Liquid/ Solid Fluidized Beds for Newtonian and Non-Newtonian Fluids

Aghajani, Masoud*[+]

Faculty of Petroleum Engineering, Petroleum University of Technology, Ahwaz, I.R. IRAN

Müller-Steinhagen, H.

Institute for Thermodynamics & Thermal Engineering, University of Stuttgart, GERMANY

Jamialahmadi, Mohammad

Faculty of Petroleum Engineering, Petroleum University of Technology, Ahwaz, I.R. IRAN

ABSTRACT: *The excellent performance of fluidized bed heat exchangers is due to the interaction between particles and heat transfer surface and to the mixing effects in the viscous sublayer. In this paper, the results of experimental investigations on heat transfer for a wide range of Newtonian and non-Newtonian (shear-thinning power law) fluids are presented. New design equations have been developed for the prediction of heat transfer coefficient. The predictions of these correlations and of numerous correlations recommended by other authors are compared with a large database compiled from the literature.*

KEY WORDS: *Fluidized bed, Non-Newtonian fluid, Heat transfer, Bed voidage*

INTRODUCTION

Liquid/solid fluidized beds are used throughout the process industry for hydrometallurgical operations, catalytic cracking, crystallization and sedimentation. In recent years, liquid/solid fluidized beds also find increasing applications in the treatment of aqueous wastes, heavy oil cracking, polymerization, biotechnology, fermentation, and food processing. Here, the liquid phase is viscous with non-Newtonian behavior. Several methods have been developed during the past years to reduce the formation of deposits in heat exchangers by chemical or mechanical means. One of the most promising concepts is the fluidized bed heat exchanger.

To apply fluidized bed heat exchangers more widely, one has to be able to predict the heat transfer coefficient for a given condition through the knowledge and understanding of the mechanisms involved. Investigations on the hydrodynamic behaviour of Newtonian systems have been documented and discussed by Jamialahmadi and Müller-Steinhagen [1].

The aim of the present investigation is, to measure the heat transfer parameters over a wide range of particle

* *To whom correspondence should be addressed.*
+ *E-mail*: *m.aghajani@ put.ac.ir*
1021-9986/04/1/119 12/$/3.2

size, density and shape using liquids with Newtonian and non-Newtonian behavior. The predictions of various published correlations are compared with these experimental data and new correlations and methodologies are presented for the predictions of the heat transfer coefficient in beds which are fluidized with Newtonian and non-Newtonian liquids.

EXPERIMENTAL EQUIPMENT AND PROCEDURE

Test Rig for Measuring Heat Transfer Coefficients

A schematic diagram of the apparatus used in this investigation is shown in Fig. 1. The test rig was completely made from stainless steel. The liquid flows in a closed loop consisting of temperature controlled storage tank, pump, liquid flow meter, control valves, and test section for heat transfer, which is shown in Fig. 2.

A 70-mash stainless steel screen fitted between two flanges before the test section supports the solid particles. The fluid temperature in the fluidized test section was measured with thermocouples appropriately located in the pipes. The flow meter was calibrated for different solutions at different bulk temperatures. The particles were prevented from carryover, at higher superficial liquid velocities, by an expansion cone mounted on top of the heated section. Power was supplied to the test section using a manually adjusted variac. A personal computer was used for data acquisition. Various types of spherical and cylindrical particles were used as solid phase in this investigation. The physical properties of the particles are listed in Table 1.

Test Liquids

In order to cover a wide range of particle Reynolds numbers, a series of aqueous solutions of sugar and carboxymethylcellulose (CMC) were used as Newtonian and non-Newtonian liquids. As expected, the sugar solutions exhibited a constant shear viscosity whereas the CMC solutions display varying levels of pseudoplastic

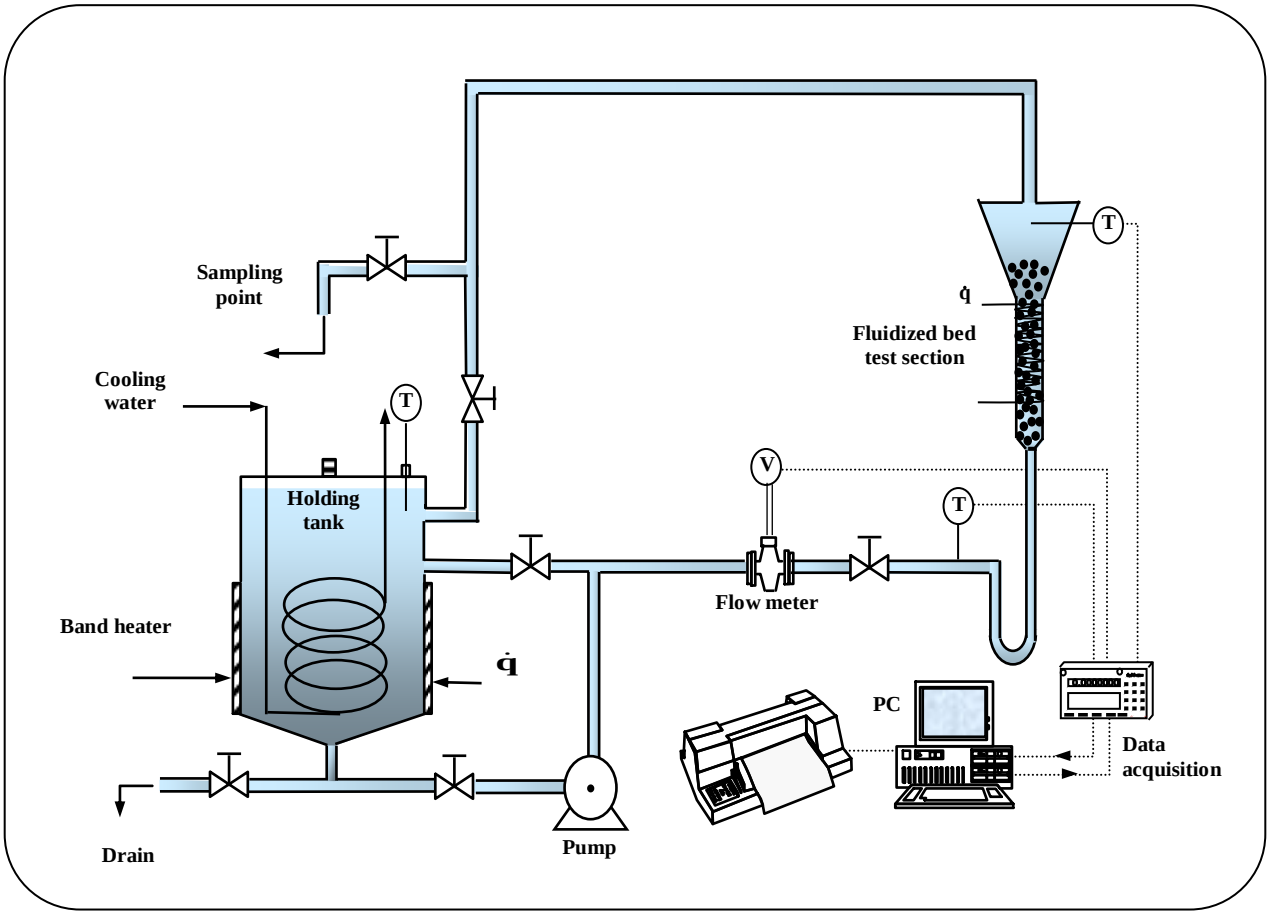

Fig. 1: Schematic diagram of test apparatus

Table 1: Physical properties of Solid particles

Type	Name	d_p or d_{pe}* [mm]	ε_{SB} [-]	Ψ [-]	Density [kg / m^3]	Specific heat [J/kg K]	Conductivity [W/m K]
Cylindrical	Aluminium 2×3 mm	2.62	0.40	0.86	2600	896	204
	Aluminium 3×3 mm	3.43	0.41	0.87	2600	896	204
	Brass 3×3 mm	3.43	0.41	0.87	8500	385	111
	Stainless Steel 3×3 mm	3.43	0.41	0.87	7900	460	17
	Stainless Steel 2×2 mm	2.29	0.40	0.87	7900	460	17
	Tantalum 4×4 mm	4.58	0.41	0.87	17600	151	54.4
Spherical	Glass	2	0.39	1	2700	840	0.87
	Glass	3	0.39	1	2700	840	0.87
	Glass	4	0.40	1	2700	840	0.87
	Lead	2.9	0.39	1	11350	130	35
	Lead	4	0.40	1	11350	130	35
	Carbon Steel	4	0.40	1	7800	473	43
	Carbon Steel	3	0.39	1	7800	473	43
	Stainless Steel	3.7	0.40	1	8100	460	13

* *d_{pe} = Equivalent diameter for cylindrical particle = Diameter of a sphere having the same volume as the particle (volume diameter).*

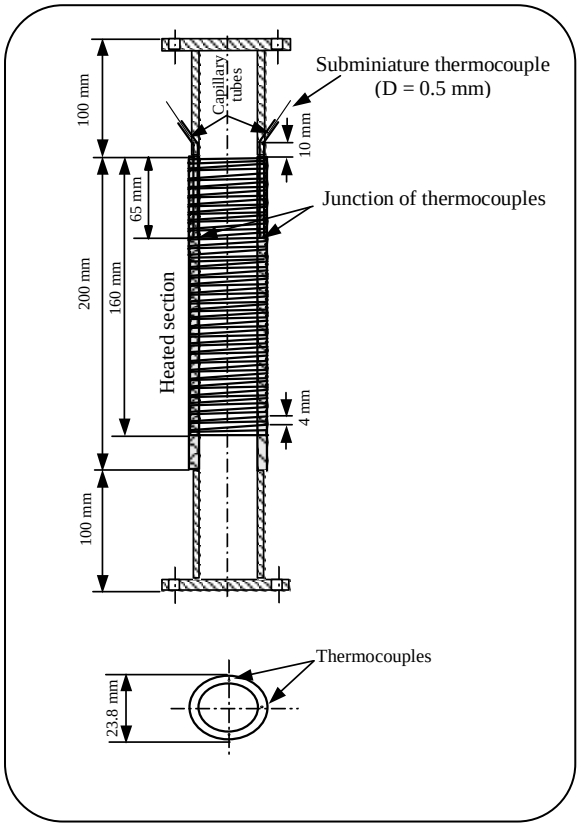

Fig. 2: Schematic of fluidized bed test section

behavior. An examination of the steady shear stress-shear rate data suggested that the two-parameter power law fluid model provides an adequate representation of their pseudoplastic behavior. For steady shear, the power law is written as:

$$\tau = k\dot{\gamma}^{n} \tag{1}$$

where the best values of k and n were estimated using a nonlinear regression approach. The resulting values along with the density of each solution are given in Table 2. It has been assumed that the average shear rate over the entire particle surface is u_∞/d_p. With this definition, the apparent viscosity is given by the following equation:

$$\mu_a = k\left(\frac{u_\infty}{d_p}\right)^{n-1} \tag{2}$$

Procedure for Measuring Heat Transfer Coefficient

The local heat transfer coefficient is defined as:

$$\alpha = \frac{\dot{q}}{T_s - T_b} \tag{3}$$

where the surface temperature, T_s, is calculated as shown in the previous section. The bulk temperature, T_b, at the

Table 2: Physical properties of test liquids

Newtonian liquids	Viscosity [Pa.s]				Density [kg / m^3]	Specific heat [J/kg K]	Conductivity [W/m K]
	25 °C	40 °C	60 °C	80 °C			
Pure water	0.0010050	0.0006560	0.0004688	0.0003565	998.3	4182	0.6
Sugar solutions						*	*
20 wt%	0.001714	0.001197	0.000811	0.000592	1070	1523	0.580
40 wt%	0.005359	0.003261	0.001989	0.001339	1150	1314	0.456
60 wt%	0.044410	0.021300	0.009870	0.005420	1300	1184	0.391

Aqueous solutions of CMC (non-Newtonian liquids)

Density ≅ Density of pure water

Power law model: $\tau = k(\dot{\gamma})^n$ where k = Viscosity coefficient, [$Pa.s^n$] & n = Rate index, [-]

CMC solutions	Power Law parameters	25 °C	40 °C	50 °C	60 °C	70 °C	Specific heat [J/kg K]	Conductivity [W/m K]
0.2 wt%	k	0.0697	0.0221	0.0125	0.0082	0.0031	4200	0.615
	n	0.7468	0.8281	0.8879	0.9233	0.9512		
0.4 wt%	k	0.2084	0.066078	0.03737	0.02452	0.00927	4220	0.625
	n	0.6953	0.770993	0.82667	0.85963	0.8856		
0.6 wt%	k	0.3413	0.108217	0.06121	0.04015	0.01518	4250	0.635
	n	0.6883	0.763231	0.81835	0.85097	0.87669		
0.8 wt%	k	0.5756	0.182507	0.10323	0.06772	0.0256	4270	0.64
	n	0.6729	0.746155	0.8012	0.83193	0.85707		
1 wt%	k	2.538	0.804732	0.45516	0.29859	0.11288	4290	0.645
	n	0.5519	0.611982	0.65618	0.68234	0.70296		

* *International Critical Tables, Vol. 5, 1929.*

thermocouple location was obtained from the following equation to account for the heater geometry.

$$T_b = T_{b,in} + \frac{95}{160}\left(T_{b,out} - T_{b,in}\right) \quad (4)$$

This assumes that the bulk temperature increases linearly, from $T_{b,\ in}$, to $T_{b,\ out}$ of the heated section. For the boundary condition of a constant heat flux this is a valid assumption.

Experiments for measuring heat transfer coefficients were performed for different bulk temperatures. All measurements were taken after the system had reached steady state conditions.

From the results of this study and also from previous investigations it has been found that in the convective heat transfer regime, the heat transfer coefficient is almost independent of the heat flux. Therefore, all experiments were performed under identical operational conditions and in the convective heat transfer regime. The range of experimental parameters used for measuring heat transfer coefficient is given in Table 3.

RESULTS AND DISCUSSION

Velocity–Voidage Relationship

Theoretical and empirical correlations available for the prediction of heat transfer coefficients are strong functions of the bed voidage. Therefore, accurate knowledge of this relationship is crucial for the reliable estimation of heat transfer coefficient. Jamialahmadi and Müller-Steinhagen [2] compiled the published correlations and conditions for which their application has been recommended. Most of these correlations are empirical and apply only over a restricted range of Reynolds number, for specific particles or for Newtonian fluids. Furthermore, the prediction of bed voidage requires the use of iterative solutions for most of these

Table 3: Range of experimental parameters for the measurements of heat transfer coefficients

d_p / D_h	0.12 to 0.17
ρ_p	2600 to 11350 kg/m^3
ρ_l	998 to 1300 kg/m^3
μ_l	0.00036 to 0.14 Pa. s
Re_p	0.12 to 1570
Ar	99 to 3.4×10^7
Pr	1.5 to 900

correlations. Therefore, in this work the bed voidages were calculated according to a new model that has been suggested by Aghajani, M., [3].

$$\varepsilon = \left(\frac{u_s}{u_t}\right)^{\frac{1}{z}} (1 - \varepsilon_{SB}) + \varepsilon_{SB} \qquad (5)$$

The static bed voidage ε_{SB} in equation (5) can be calculated by the following equations.

For spherical particles:

$$\varepsilon_{SB} = \frac{0.15}{\left(\frac{D_h}{d_p} - 1\right)} + 0.38; \ \frac{D_h}{d_p} \geq 2.033 \qquad (6)$$

For cylindrical particles:

$$\varepsilon_{SB} = \frac{0.15}{\left(\frac{D_h}{d_p} - 1\right)} + 0.39 \ ; \ \frac{D_h}{d_p} \geq 2.033 \qquad (7)$$

and the fluidization index, z can be calculated by the following equation.

$$z = \frac{0.65(2 + 0.5\,Re_{p\infty}^{0.65})}{(1 + 0.5\,Re_{p\infty}^{0.65})} \qquad (8)$$

Heat Transfer

Heat transfer measurements have been obtained for single-phase flow and two-phase liquid/solid fluidized beds in a cylindrical tube using Newtonian and non-Newtonian shear-thinning power law) solutions and a variety of cylindrical and spherical particles at different bulk temperatures. Significant increases in heat transfer were observed due to the presence of the suspended solids as shown in Fig. 3 (a, b and c) for fluidization with Newtonian and non-Newtonian liquids. At low flow velocities, the solid particles lie on top of each other and

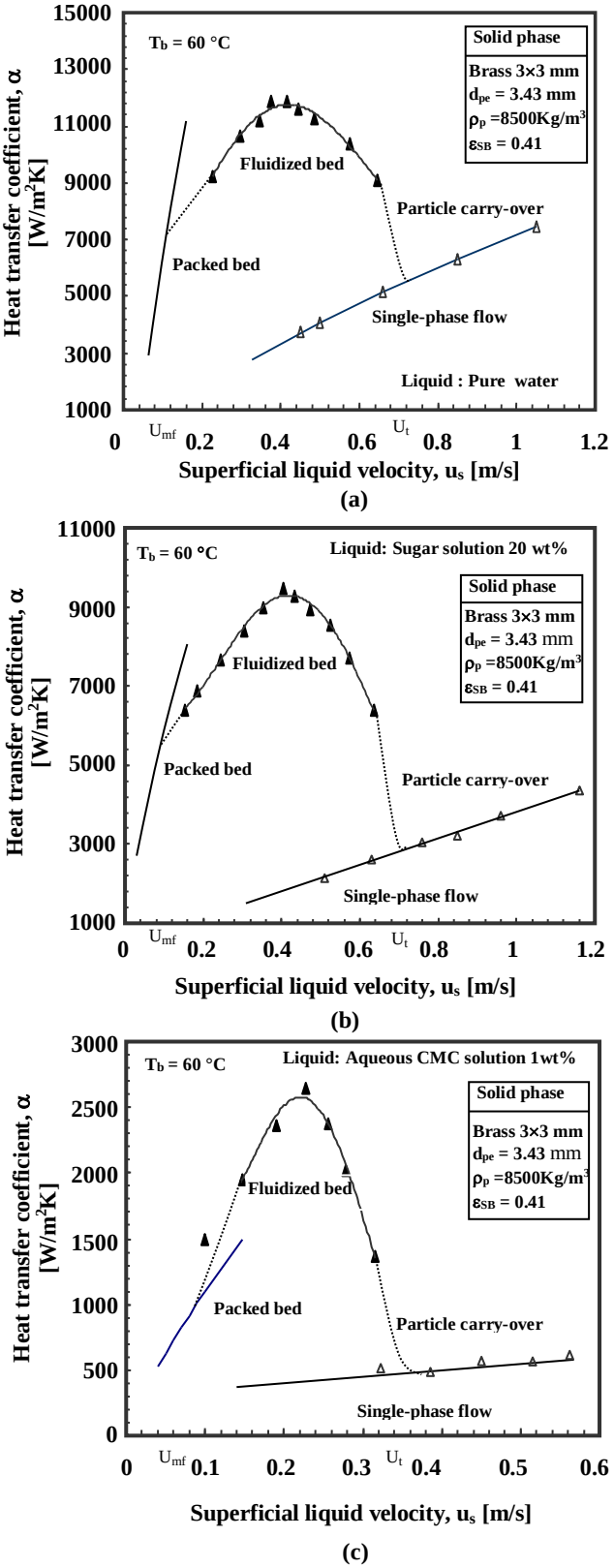

Fig. 3: Heat transfer coefficients for packed bed, fluidized bed and single-phase flow versus liquid velocity for fluidization with (a) and (b), Newtonian and (c), non-Newtonian liquids

on the porous bottom of the column and the bed is in a packed bed state. When the superficial liquid velocity exceeds the minimum fluidization velocity, u_{mf} fluidization starts. By further increase of superficial liquid velocity, the heat transfer coefficient, α increases up to a maximum value. Then, the heat transfer coefficient decreases, reaching the single-phase value at terminal velocity, u_t. At high flow velocities the solid particles are conveyed out of the column. It is found that heat transfer coefficients for liquid/solid fluidized bedsare up to 7 times higher than for single-phase flow at the same velocity. For fluidization with high viscosity Newtonian or non-Newtonian liquids this increase in heat transfer coefficient is lower. A Possible reason is low movement of particles in high viscosity solutions. Therefore the contribution of this mechanism to enhancement of heat transfer coefficient becomes lower. For packed beds in these figures the heat transfer coefficient is calculated using the Yagi and Wakao [4] equation:

$$Nu_p = 0.20\,Re_p^{0.8}\,Pr^{1/3} \qquad (9)$$

Comparison of Measured Heat Transfer Coefficients with Previously Published Models

To discuss the trends predicted by the different correlations, measured heat transfer coefficient for 2.9 mm lead particles are used. Typical results of the comparison between the measured and calculated heat transfer coefficients are shown in Figs. 4 and 5. Most correlations show the maximum in the heat transfer coefficient. However, the variation between the predictions of the different correlations is quite considerable.

Development of a New Heat Transfer Model

Based on the findings of this study and also previous investigations, heat transfer to/from liquid/solid fluidised beds must be influenced by the intensity of the interchange between the solid particles and the heater surface, which is a function of the velocity of the particles and the frequency and density of particle contact with the heater surface. Hence, a new model has been formulated based on the following assumptions.

(I) The major resistance to heat transfer is a liquid film near the heat transfer surface.

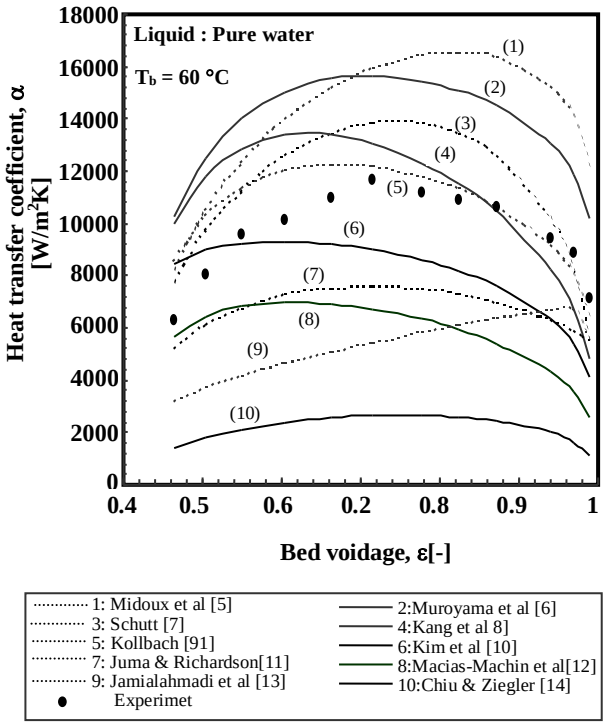

Fig. 4: Comparison of measured and predicted heat transfer coefficients for 2.9 mm lead Particles fluidized in Newtonian liquid.

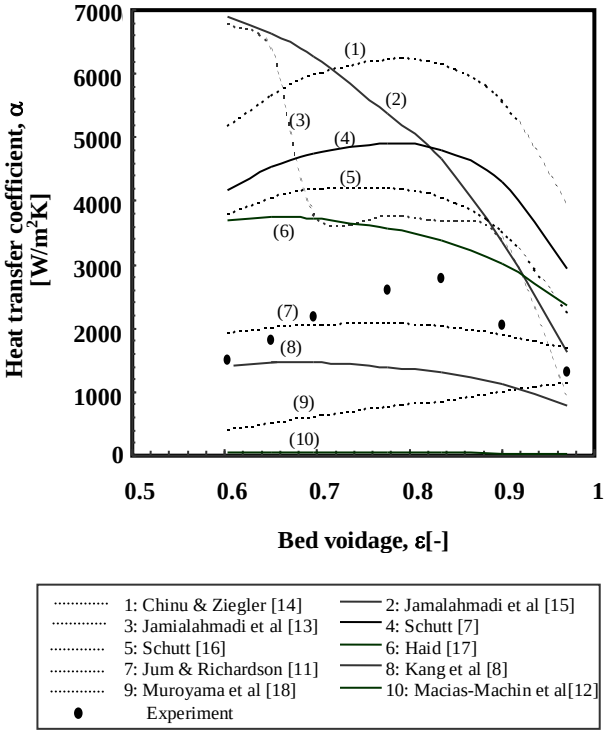

Fig. 5: Comparison of measured and predicted heat transfer coefficients for 2.9 mm lead particles fluidized in non-Newtonian liquid.

(II) Due to the movement of solid particles there is a steady flow of fluid elements from the bulk of the fluid to the heat transfer surface and vice versa. The fluid elements reside for a finite time at the surface until they return to the bulk in the wake of solid particles scouring the heat transfer surface. In this region heat is transferred into the fluid by transient heat conduction from the heat transfer surface. Some heat is also transferred by conduction to the particles while they are in contact with the heat transfer surface.

(III) On these parts of the heat transfer surface that are not in contact with particles, heat is transferred to the liquid by forced convection.

Therefore heat transfer at any moment is component of two parallel mechanisms in separate zones of the heat transfer surface i.e. the surface area affected by particles, A_p, and the remaining heat transfer area, A_c, in which heat is transferred by forced convection.

Han and Griffith [19] have shown that the area from which the hot liquid layer is pumped away by a vapour bubble leaving the heat transfer surface is πd_b^2. Since small bubbles and solid particles behave similarly, the area of the heat transfer surface affected by a single particle should also be πd_p^2. The following approach is hence analogous to nucleate boiling heat transfer if "vapour bubble" is replaced by "particle" and "latent heat transfer" by "particle conduction".

Time-averaged heat transfer coefficients may be additive if it is assumed that both mechanisms (heat transfer by fluid convection and heat transfer by transient heat conduction from the heat transfer surface) coexist over the entire heat transfer surface. Therefore, the total heat transfer coefficient α is:

$$\alpha = \alpha_c + \alpha_p \tag{10}$$

The local forced convective heat transfer coefficient, α_c, can be calculated from the Gnielinski [20] equation for heat transfer during turbulent flow in pipes if it is modified to apply for local conditions.

$$Nu = \frac{\frac{f_i}{8}(Re-1000)Pr}{1+12.7\sqrt{\frac{f_i}{8}}\left(Pr^{2/3}-1\right)}\left[1+\frac{1}{3}\left(\frac{D}{X}\right)^{2/3}\right]\left(\frac{Pr_b}{Pr_w}\right)^{0.11} \tag{11}$$

Based on extensive experimental and numerical research Jamialahmadi and Müller-Steinhagen [15] suggested using Re instead of (Re–1000) in equation 11. The friction factor, f_i for turbulent flow may be calculated according to Filonenko [21].

$$f_i = \left[1.82\,Log(Re) - 1.64\right]^{-2} \tag{12}$$

An average relative error of 5.7% for Newtonian solutions and 8.6% for non-Newtonian (shear thinning power law) solutions indicated that there is very good agreement between the measured data and the predictions of the modified Gnielinski [20] equation.

Prediction of α_p

The heat transfer coefficient for the particle-controlled area, α_p also includes two parallel heat transfer coefficients

$$\alpha_p = \alpha_{wl} + \alpha_{wp} \tag{13}$$

In the above equation α_{wl} is the heat transfer coefficient from the wall to the adjacent liquid layer and α_{wp} is the heat transfer coefficient from the wall to the particle. Following the departure of the particle and the hot liquid layer, the liquid at T_b from the main body of the fluid flows into the area of influence πd_p^2 and comes into contact with the heating surface at T_w. Assuming pure conduction into the liquid and particle in the area of the influence, this part of problem can be modeled as conduction to a semi-infinite liquid with a step change in temperature ($\Delta T=T_w-T_b$) at the surface.

$$\frac{q_p}{A} = \frac{\sqrt{\lambda\rho c}\,\Delta T}{\sqrt{\pi t}} \tag{14}$$

The hot layer is replaced with a frequency f, which is equal to the frequency of the collision of particles with the heat transfer surface. Hence, similar to the study of Mikic and Rohsenow [22] on pool boiling, the average heat flux over the area of influence would be:

$$\dot{q}_p = \frac{2\sqrt{\lambda_l \rho_l c_{p,l}}\,\sqrt{f}\,\Delta T}{\sqrt{\pi}} \tag{15}$$

Taking into account the heat transfer to the particles by conduction when they are in contact with the heat transfer surface, the equation (15) can be written as:

$$\dot{q}_p = \left(\frac{2}{\sqrt{\pi}}\sqrt{\lambda_l \rho_l c_{p,l}} + \pi d_p^2 \sqrt{\lambda_p \rho_p c_{p,p}}\right)\sqrt{f}\,\Delta T \tag{16}$$

Therefore, the heat transfer coefficient for the

particle-controlled area can now be obtained from thefollowing equation.

$$\alpha_p = \left(\frac{2}{\sqrt{\pi}} \sqrt{\lambda_l \rho_l c_{p,l}} + \pi d_p^2 \sqrt{\lambda_p \rho_p c_{p,p}} \right) \sqrt{f} \qquad (17)$$

In the above equations, f is equal to the frequency of particles approaching the heat transfer surface. By analogy to the kinetic theory of gases (applied to the randomly moving solid particles in a fluidized bed) Martin [23], [24] has shown that:

$$f = \frac{1}{t_c} = \frac{Cu_p}{4d_p} \qquad (18)$$

Where C is a constant between 2 and 4 for gas and liquid fluidizations. Determining the particle velocity, u_p in fluidized beds is difficult and would require special equipment. Many of investigators such as Latif and Richardson [25] have speculated that in fluidized beds the particle velocity is proportional to the superficial liquid velocity and at $\varepsilon=\varepsilon_{SB}$ it must be zero. Therefore, it is assumed that:

$$u_p = m u_s (\varepsilon - \varepsilon_{SB})^a \qquad (19)$$

Considering that particle contact frequency must be zero at $\varepsilon = 1$, using equation (19), equation (18) may be modified to:

$$f = K \left(\frac{u_s}{d_p} \right) (\varepsilon - \varepsilon_{SB})^a (1-\varepsilon)^b \qquad (20)$$

In above equations m, K, a, and b are constants. By analyzing a huge number of experimental data for both Newtonian and non-Newtonian liquid-solid fluidized beds it was found that good agreement with experimental data was obtained as following:

For Newtonian liquid-solid fluidized beds:

$$f = 2 \left(\frac{u_s}{d_p} \right) (1-\varepsilon)^{1.8} (\varepsilon - \varepsilon_{SB})^{0.2} \qquad (21)$$

For non-Newtonian liquid-solid fluidized beds:

$$f = 0.9 \left(\frac{u_s}{d_p} \right) (1-\varepsilon)^{1.8} (\varepsilon - \varepsilon_{SB})^{1.6} \qquad (22)$$

In this investigation both particulate and aggregative fluidization behavior is occurring and from the presented model it is obvious that the heat transfer coefficient depends into collision frequency of contacting particles, f given by equations 21 and 22 and according to these equations it relates to the bed voidage and hence to the hydrodynamics of system.

The collision frequency of contacting particles with heat transfer surfaces, f must increase from zero for a packed bed up to a maximum value, at some superficial liquid velocity, before decreasing to zero for single-phase flow. The collision frequency calculated in the present model given by equations 21 and 22 is zero for packed or static beds and for single-phase fluid flow, and generally reaches a maximum for a bed voidage between 0.65 and 0.85, in accordance with the maximum heat transfer coefficient. Moreover, it is clear that the contact frequency is affected by the viscosity of the liquid and as can be seen in the Fig. 6 for fluidization in highly viscous liquids (in which the fluidization behavior tends to be particulate) it significantly decreases.

Comparison of Published Heat Transfer Coefficients with the Present Model

In the experimental part of this work, a large number of data over a wide range of possible operating parameters have been obtained for heat transfer in liquid/solid fluidized beds with Newtonian and non-Newtonian liquids. These data have been complemented by all the published data the authors could extract from the literature. Checking for consistency, all data for velocities greater than the terminal velocity or data sets where the measured In the experimental part of this work, a large number of data over a wide range of possible operating parameters have been obtained for heat transfer in liquid/solid fluidized beds with Newtonian and non-Newtonian liquids. These data have been complemented by all the published data the authors could extract from the literature. Checking for consistency, all data for velocities greater than the terminal velocity or data sets where the measured wall temperatures were outside the fluidised region were removed.

Typical predictions of the present model for different particles fluidized in Newtonian and non-Newtonian solutions are shown in figs. 7 and 8. The calculated trends are in excellent agreement with the experimental data of this study and of all previous investigators. The applicability of the present model for Newtonian and non-Newtonian liquid/solid fluidized beds is demonstrated in Figs. 9 and 10 where the experimental

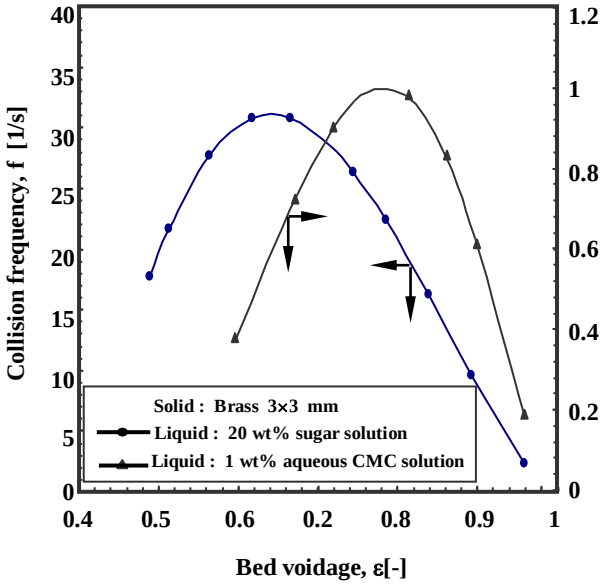

Fig. 6: Collision frequency, f, as a function of bed voidage ε

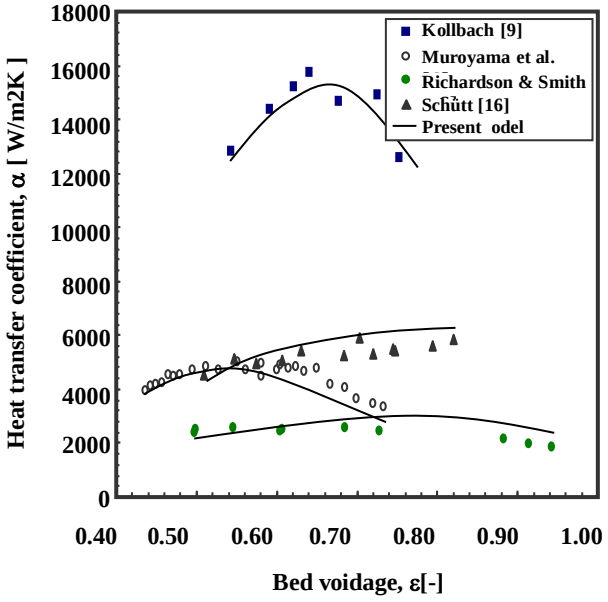

Particles	Liquid	ρ_p (kg/m^3)	T_b (°C)
Stainless steel 2×2 mm	Pure water	7900	94
Glass 3.1 mm	Pure water	2500	40
Gravel 1.8 mm	Pure water	2670	15
Glass 2.5 mm	Pure water	2500	80

Fig. 7: Comparison of measured and predicted heat transfer coefficients for fluidization in a Newtonian liquid.

data of this study and of various other investigators are compared with those predicted from the model presented in this investigation.

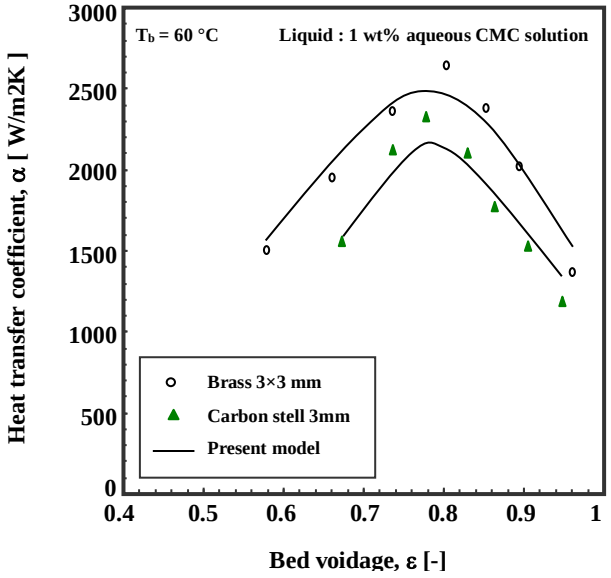

Fig. 8: Comparison of measured and predicted heat transfer coefficients for fluidization in a non-Newtonian liquid

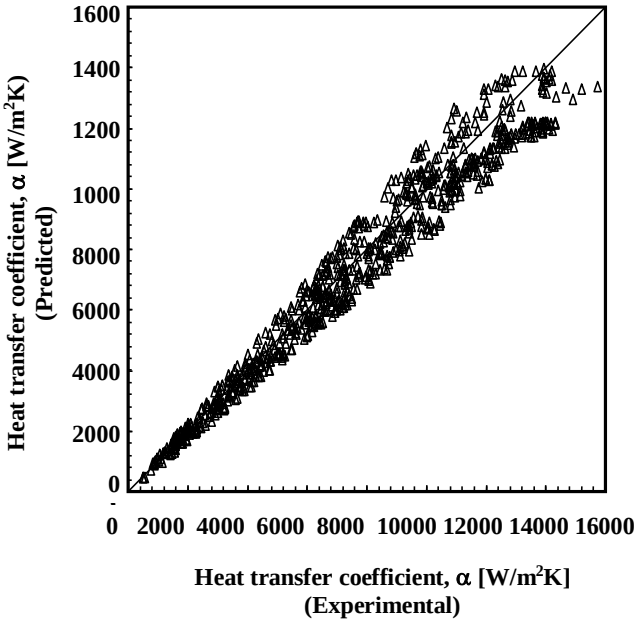

Fig. 9: Comparison of measured and predicted heat transfer coefficients with values calculated from the present model for Newtonian liquids

The average relative errors $\left|\Delta_{rel}\alpha\right|_{av}$ and the standard deviation of prediction,σ, of typical correlations used in this comparison, which are defined as follows, are shown in Table 4

Table 4: Typical comparison of measured data and values predicted by published models.

No.	Author	*Newtonian Liquids*			*Non-Newtonian Liquids*		
		average relative error (%)	Standard deviation (%)	Prediction	average relative error (%)	Standard deviation (%)	Prediction
1	Kollbach [9]	38.6	15.3	±	80.2	58.3	+ +
2	Schütt [16]	46.8	16.9	±	94.2	70.7	+
3	Juma & Richardson [11]	41.7	19.6	–	44	42.2	±
4	Kang et al. [8]	38.7	21.5	±	32.2	32.8	±
5	Kim et al. [10]	30.7	14.5	–	52.6	57.3	±
6	Jamialahmadi et al. [15]	35.8	16.3	±	189	216	±
7	Muroyama et al. [6]	43	27.3	±	38.2	34.5	±
8	Schütt [7]	46	23.2	±	152.2	93.1	+ +
9	Macias-Machin et al. [12]	47	31.7	– –	88.6	4.4	– –
10	Jamialahmadi et al. [13]	39.3	16.7	±	123	194	+ +
11	Chiu & Ziegler [14]	78.6	16.6	– –	249	126	+ +
12	Muroyama et al. [18]	45.3	32.2	±	45.5	48.2	±
13	Haid [17]	36.7	22.4	±	135.5	83	+ +
14	Grewal & Zimmermann [27]	38.1	28	±	138	131	+
15	Present model	12.8	14.5	±	15.3	14.1	±

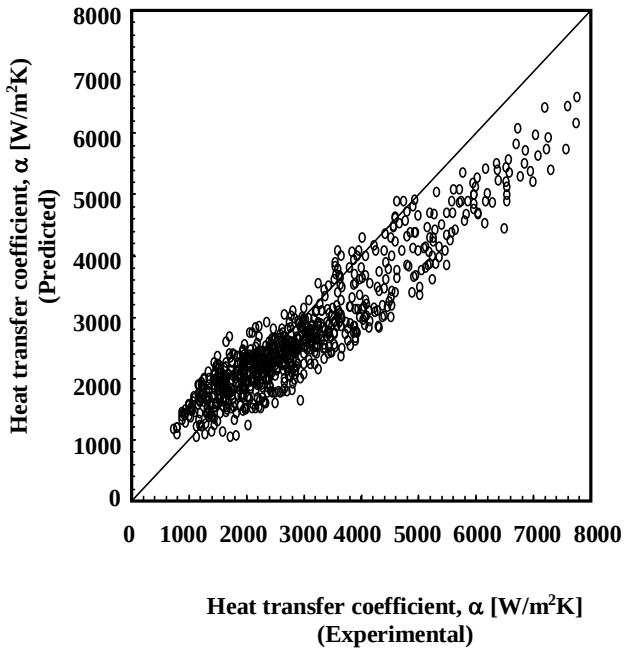

Fig. 10: Comparison of measured and predicted heat transfer coefficients with values calculated from the present model for non-Newtonian liquids

Relative error, $|\Delta_{rel}\alpha| = \left|\left(\alpha_{cal} - \alpha_{exp}\right)/\alpha_{exp}\right| (\%)$

Average relative error, $|\Delta_{rel}\alpha|_{av} = \Sigma|\Delta_{rel}\alpha|/n \quad (\%)$

n = number of data sets

Standard deviation, $\sigma = \left(\Sigma\left(|\Delta_{rel}\alpha| - |\Delta_{rel}\alpha|_{av}\right)^2/n\right)^{0.5} (\%)$

n = number of data sets

Comparing the average relative errors and the standard deviation of predicted values for all published correlations and of the present model, it is evident that the model developed in the present investigation provides better results than all other correlations. This table also indicates whether correlations tend to underpredict "–" or overpredict "+" the measurements. Correlations with "– – " or "+ + " have a high tendency to underpredict or overpredict the measurements, and for correlations with "± " no clear tendency was found.

Compared with the other correlations, the present model for Newtonian and non-Newtonian liquids provides better results than all other models and correlations.

CONCLUSIONS

New model are presented for heat transfer coefficient for liquid/solid fluidized beds in vertical pipes. This mechanistic model takes into consideration the forces acting on the particles as well as the interaction between heat transfer surface and fluidized particles. It is applicable for both Newtonian and non-Newtonian liquids. Comparison with substantial data bank with data from various authors indicates that the presented model outperforms previously published correlations.

Nomenclature

A	Heat transfer surface area	m^2
A_c	Surface area affected by forced convection	m^2
A_p	Surface area affected by particle	m^2
a, b	exponents	–
C	Coefficient	–
C_P	Heat capacity	J/ kg. K
d_b	bubble diameter	m
d_P	Particle diameter	m
D	Diameter of fluidized bed	m
D_h	Hydraulic diameter of fluidized bed	m
F	Collision frequency	s^{-1}
f_i	Friction factor	–
k	Viscosity coefficient	$Pa.s^n$
K	Coefficient	–
M	Coefficient	–
N	Number of data sets	–
$\dot{q}$	Heat flux	W/m^2
T	Temperature	K
t_c	Contact time	s
u_p	Particle velocity	m/s
u_s	Superficial liquid velocity	m/s
u_t	Particle terminal velocity corrected for wall effect	m/s
u_∞	Particle terminal velocity in an infinite fluid	m/s
X	Length in flow direction	m
z	Fluidization index	–

Greek letters

α	Heat transfer coefficient	W/m^2. K
ε	Bed voidage	–
λ	Thermal conductivity	W/m. K
μ	Dynamic viscosity	kg/m. s
σ	Standard deviation	–
ρ	Density	kg/m^3
τ	Shear stress	Pa. S^n
ψ	shape factor	–
$\dot{\gamma}$	Shear rate	s^{-1}
μ_a	Apparent viscosity	kg/m. s

Subscripts-Superscripts

a	Apparent
av	Average
b	Bulk
c	Forced convection
cal	Calculated
exp	Experimental
l	Liquid
n	Rate index
p	Particle
rel	Relative
s	Solid
SB	Static bed
W	Wall
Wl	Wall to adjacent liquid
Wp	Wall to the particle

Dimensionless groups

Ar	Archimedes number	$gd_P^3 (\rho_s - \rho_l) \rho_l / \mu_l^2$
Nu	Nusselt number	$D\alpha / \lambda_l$
Pr	Prandtl number	$\mu_l Cp_l / \lambda_l$
Re	Reynolds number	$\rho_l U_s D / \mu_l$
$Re_{p\infty}$	Particle terminal Reynolds number In an infinite liquid	$u_\infty d_P / \nu_l$

Received: 20th July 2003 ; Accepted: 21st October 2003

REFERENCES

[1] Jamialahmadi, M. and Müller-Steinhagen, H., Hydrodynamics and Heat Transfer of Liquid Fluidized Bed Systems, *Chem. Eng. Comm.*, **179**, pp.35-79, (2000).

[2] Jamialahmadi, M. and Müller-Steinhagen, H., Bed Voidage in Annular Solid-Liquid Fluidized Beds, *Chemical Engineering and Processing*, **31**, pp. 221-227, (1992).

[3] Aghajani, M., Studies of Bed Voidage and Heat Transfer in Solid-Liquid Fluidized Bed Heat

Exchangers, PhD thesis, University of Surrey, UK, (2001).

[4] Yagi, S. and Wakao, N., Heat and Mass Transfer from Wall to Fluid in Packed Beds, *AICHE J*., **5**, pp. 79-85, (1959).

[5] Midoux, N., Wild, J., Purwasamita, M., Chapentier, J. C. and Martin, H., Zum Flüssigkeitsinhalt und zum Wärmeübergang in Rieselbettreaktoren bei boher Wechselwirkung des Gases und der Flüssigkeit, *Chem. Eng. Tech.*, **58**, pp. 142-143, MS1445/86, (1986).

[6] Murayama, K., Fuluma, M. and Yasunishi, A., Wall-to-Bed Heat Transfer in Liquid-Solid and Gas-Liquid-Solid Fluidized Beds, *Can. J. Chem. Eng.*, **64**, pp. 399-408, (1986).

[7] Schütt, U., Wärmeübertragung in der Flüssigkeitswirbelschicht mit senkrechten Rohren, Wiss Zeitung der Techn. Hochschule Magdeburg, **26**, pp. 71-74, (1982).

[8] Kang, Y., Fan, L.T. and Kim, S. D., Immersed Heater-Type Bed Heat Transfer in Liquid-Solid Fluidized Beds, *AIChE J.*, **37**, pp. 1101-1106, (1991).

[9] Kollbach, J., Ph. D. Thesis, Universität Achen, Achen, (1987).

[10] Kim, S. D., Kang, Y. and Kwon, H. K., Heat Transfer Characteristics in Two and Three Phase Slurry Fluidized Beds, *AIChE J*., **32**, pp. 1397-1400, (1986).

[11] Juma, A. K. A. and Richardson, J.F., Heat Transfer to Cylinders from Segregating Liquid-Solid Fluidized Beds, *Chemical Engineering Science*, **40**, pp. 687-694, (1985).

[12] Macias-Machin, A., Oufer, L. and Wannenmacher, N., Heat Transfer between an Immersed Wire and a Liquid Fluidized Bed, *Powder Technology*, **66**, pp. 281-284, (1991).

[13] Jamialahmadi, M., Malayeri, M. R., and Mülller-Steinhagen, H., A Unified Correlation for the Prediction of Heat Transfer Coefficients in Liquid-Solid Fluidized Bed Systems, *Journal of Heat Transfer*, **118**, pp. 952-959, (1996).

[14] Chiu, T. M. and Ziegler, E. N., Liquid Hold-up and Heat transfer Coefficient in Liquid-Solid and Three-Phase Fluidized Bed, *AIChE J.*, **31**, pp.1504-1509,(1985).

[15] Jamialahmadi, M. and Müller-Steinhagen, H., "Forced Convective and Subcooled Flow Boiling Heat Transfer to Spent Bayer liquor", Light Metals, pp. 141-150, (1992).

[16] Schütt, U., Wärmeübertragung in der Flüssigkeitswirbelschicht mit senkrechten Rohren, Ph. D. Thesis, Universität Magdeburg, (1983).

[17] Haid, M., Martin, H. and Müller-Steinhagen, H., Heat Transfer to Liquid-Solid Fluidized Beds, *Chem. Eng. and Processing*, **33**, pp. 211-225, (1994).

[18] Murayama, K., Fuluma, M. and Yasunishi, A., Wall-to-Bed Heat Transfer in Gas- Liquid-Solid Fluidized Beds, *Can. J. Chem. Eng.*, **62**, pp. 199-208, (1984).

[19] Han, C. Y., and Griffith, P., The Mechanism of Heat Transfer in Nucleate Pool Boiling, Part I and II, *int. J. Heat and Mass Transfer*, **8**, pp. 887-917, (1965).

[20] Gnielinski, V., "Wärmeübergang in Rohren", VDI-Wärmeatlas, 5th ed., VDI-Verlag, Düsseldorf, (1986).

[21] Filonenko, G. K., Hydraulic Resistance in Pipes, *Teploenergetika*, **1**, pp. 40-44, (1954).

[22] Mickic, B. B., and Rohsenoe, W. M., A New Correlation of Pool Boiling Data Including the Effect of Heat Surface Characteristics, *J. Heat Transfer*, **5**, pp.245-250 , (1969).

[23] Martin, H., Fluid Bed Heat Exchangers- A New Model for Particle Convection Energy Transfer, *Chem. Eng. Commun.*, **13**, pp. 1-16, (1981).

[24] Martin, H., " Fluidized Beds", Heat Exchanger Design Handbook, Hemisphere Publishing Corporation, Washington DC, pp. 2.8.4.1-2.8.4.14, (1990).

[25] Latif, B. A. J. and Richardson, J. F., Circulation Patterns and Velocity Distributions for Particles in a Liquid Fluidized Bed, *Chem. Eng. Sci.*, **72**, pp. 1933-1949, (1972).

[26] Richardson, J. F. and Smith, J. W., Heat Transfer to Liquid-Fluidized Systems and to Suspensions of Coarse Particles in Vertical Transport, *Trans. Inst. Chem. Eng.*, **40**, pp.13-22, (1962).

[27] Grewal, N. S. and Zimmerman, A. T., Heat Transfer from Tube Immersed in a Liquid-Solid Fluidized Bed, *Powder Technology*, **54**, pp. 137-145, (1988).